2011

Development and Validation of a Model to Predict Air Temperatures and Humidities in the Headspace of Partially Filled Stored Grain Silos

Johnselvakumar Lawrence, *Kansas State University*
Dirk E. Maier, *Kansas State University*

Development and Validation of a Model to Predict Air Temperatures and Humidities in the Headspace of Partially Filled Stored Grain Silos

J. Lawrence, D. E. Maier

Abstract. *During storage, headspace conditions play an important role in affecting the physical, chemical, and biological activities of living organisms in the upper layer of a grain mass. A model was developed using energy and mass balance principles to predict temperature and relative humidity of the headspace air in a partially filled silo. The formulation of the headspace domain had nine control volumes (nine temperatures and RH values) with the grain and roof surfaces as boundaries. Solar radiation and convective heat transfer were used as the driving factors for heat transfer in the headspace. Humidity transfer due to the air mass flow rate was considered the driving factor behind changes in headspace RH. The periodic changes in solar radiation and wind speed induced temperature and humidity variations in the silo headspace. The predicted results were validated using observed data. The standard error of predicted versus observed headspace air and wall temperatures was in the range of 2.3˚C to 5.3˚C and 3.1˚C to 5.5˚C, respectively. The standard error of predicted versus observed headspace humidities was around 7%. The developed model is considered sufficiently accurate and reliable to predict air temperature and relative humidity at multiple locations in the headspace of a grain storage silo.*

Keywords. *Energy and mass balance, Grain storage, Headspace, Modeling, Solar radiation.*

Bulk grain storage is an important link in the grain handling and processing supply chain. A bulk grain storage system consists of the grain mass, air, and the components of the storage structure, including the plenum or duct, the roof, and aeration fans. The confined air volume between the roof and above the grain surface is defined as the headspace. During storage, headspace air conditions play a significant role with respect to the physical, chemical, and biological activities in the grain mass. The headspace temperature is usually higher than the ambient temperature during the day and in near equilibrium with ambient temperature during the night. The higher temperature during the day is due to direct solar radiation on the wall and roof, and due to the induced natural convection currents inside the headspace. The infiltration of ambient air through eave and vents also influences the headspace air conditions. This combination of solar radiation and ambient air infiltration affects the headspace temperature and relative humidity. When the headspace temperature increases, the water holding capacity of the headspace air also increases. Moisture evaporated from the grain surface and movement of high-humidity air from the intergranular space into the headspace increases the humidity in the headspace air. Ambient air, which flows through vents and eave openings, dilutes the headspace air humidity and temperature. Improper design with insufficient ventilation may increase the temperature and humidity of the headspace air, favoring insect and mold growth. When ambient temperatures drop during evening hours, the headspace air temperature cools quickly. The decrease in temperature below the dewpoint causes the moisture in the higher RH air to condense on the underside surface of the roof and on the grain surface. The water condensed under the roof can drip onto the grain, which can lead to additional mold growth on the grain mass surface.

Knowledge of headspace temperature and humidity conditions inside the silo is essential when managing stored grain. In the past, most computer simulation models neglected the effect of headspace due to the complexity involved in modeling the headspace conditions. Researchers started modeling headspace conditions during the late 1980s. Nguyen (1987) developed a two-dimensional (2D) finite difference heat and momentum transfer model for a combined headspace and grain mass domain. This model assumed that there was no air infiltration into the headspace, i.e., it was closed in all directions in order to simplify the model. A step change in temperature based on the daily heating period was implemented on the left side of the 2D model domain as a prescribed boundary condition, and the right side was kept at a constant temperature. It was assumed that the top and bottom boundaries of the silo were insulated. This situation did not represent an actual grain storage scenario; therefore, this model lacked usefulness. Casada and Young (1994), Montross et al. (2002a), and Kaliyan et al. (2005) developed energy and moisture balance models to quantify average headspace air temperature and humidity. These models used

Submitted for review in March 2011 as manuscript number FPE 9083; approved for publication by the Food & Process Engineering Institute Division of ASABE in August 2011. Presented at the 2010 ASABE Annual Meeting as Paper No. 1009951.

Contribution No. 11-266-J from the Kansas Agricultural Experiment Station.

The authors are **Johnselvakumar Lawrence, ASABE Member,** Post-Doctoral Fellow, and **Dirk E. Maier, ASABE Member,** Professor and Head, Department of Grain Science and Industry, Kansas State University, Manhattan, Kansas. **Corresponding author:** Dirk E. Maier, Department of Grain Science and Industry, 201 Shellenberger Hall, Kansas State University, Manhattan, KS 66506; phone: 785-532-4052; fax: 1-785-532-7010; e-mail: dmaier@ksu.edu.

  ISSN 2151-0032

the fourth-order Runge Kutta method to solve these coupled equations. Casada and Young (1994) described average headspace temperature and humidity in a closed-boundary rail car carrying peanuts. Since the control volume for this model was closed, the mass flow into the headspace from the outside was not included. Headspace temperatures predicted by this model followed the trend of observed values, with the exception that the daytime peaks and nighttime valleys were underpredicted. Montross et al. (2002a) and Kaliyan et al. (2005) modified Casada and Young's model to predict headspace air conditions in ventilated grain storage silos. Montross et al. (2002a) formulated the headspace model with a system of nine ordinary differential equations: four for the headspace wall, four for the roof, and one for the headspace air. The energy and mass balance concept was used to model the plenum heat and humidity transfer with a system of five ordinary differential equations: four for the plenum wall, and one for the plenum air. Kaliyan et al. (2005) modified the Montross model by including more sections in the wall and roof. This model had a system of 17 ordinary differential equations: eight for the headspace wall, eight for the roof, and one for the headspace air. The effect of mechanical ventilation and mass flow in and out of the headspace due to thermal buoyancy was included in the model. However, the headspace air or roof or wall temperatures predicted by the model were not discussed; instead, the researchers only compared the observed headspace air temperature with ambient temperature.

The above-mentioned studies formulated the headspace and plenum models with only one temperature and relative humidity to represent the entire headspace and plenum volume. Since the headspace and plenum conditions change based on external and internal influences, the assumption of an average temperature and RH for the entire volume may not accurately represent the actual conditions inside the headspace and plenum. Montross et al. (2002a) used energy balance principles to formulate a 2D wall model. The major disadvantage of using this 2D model is that it can only have one wall temperature and in only one direction. To study the influence of the four different directions (E, W, N, S), the model has to run four different times with appropriate modifications in solar azimuth angle for each direction. In addition, the combined effect of temperature and humidity in the headspace and plenum cannot be studied using a 2D model.

Usually in silos, the temperature of the headspace air near the roof peak is higher than that near the wall due to the effect of direct solar radiation. The roof and wall in turn emit radiation that also increases the headspace air temperature. As a result, an air temperature gradient develops from the roof and wall toward the center of the headspace region as a function of the diameter and height of the silo. This difference has been observed inside the pilot silos of the Post-Harvest Education and Research Center (PHERC) at Purdue University, West Lafayette, Indiana. A temperature difference of up to 3°C to 4°C was noted during times of peak solar radiation (Lawrence, 2010). A temperature difference of 3°C to 5°C was observed between the roof region and the center region during high solar radiation (Lawrence, 2010). For large commercial and farm silos, even greater headspace temperature gradients can be expected, especially if the silos are only partially filled. Although no data are currently available, the same variability is presumed to exist with respect to relative humidity. Thus, the assumption of an average temperature and relative humidity representing the entire headspace does not appear to be realistic.

In this study, the headspace model domain was divided into multiple sections so that the temperature and RH gradients could be predicted more accurately in a partially filled stored grain silo. This more precise approach was sufficiently incorporated into a comprehensive three-dimensional (3D) stored grain ecosystem storage model.

Model Development

In a partially filled stored grain silo, a portion of the upper side wall is exposed to the headspace air. In this exposed wall scenario, the headspace has both cylindrical and conical shaped control volumes. The following assumptions were made while developing this model:

- No temperature or moisture variation occurred within the control volumes.
- The air movement within the control volume is constant.
- Constant temperature and moisture gradients exist between two volumes.
- Uniform wind speed in all directions with respect to the silo wall.

For model development, the headspace was divided into nine control volumes. The boundaries of the headspace have eight wall sections, eight roof sections (the center and side sections have a total of 16 roof sections; however, in order to reduce the number of equations, the center and side sections were taken as one section), and nine grain surface sections (fig. 1). A set of 25 non-linear transient ordinary differential equations (eqs. 1 through 4) for each section representing air, wall, and roof in the headspace domain were formulated:

$$\left[(\rho c)_a V_c \frac{dT_{H,1}}{dt} = \left(\frac{m_a}{9}\right) c_a \sum_{i=2}^{9} (T_{H,i} - T_{H,1}) + m_a c_a (T_{amb} - T_{H,1}) + \sum_{i=1}^{8} h_{ri} A_{rc,i} (T_{rf,i} - T_{H,j}) + h_g A_{g,1} (T_{g,1} - T_{H,1})\right] \quad (1)$$

$$\left[(\rho c)_a V_s \frac{dT_{H,j}}{dt} = h_g A_{g,j} (T_{g,j} - T_{H,j}) + h_{wi} A_{w,j} (T_{w,j} - T_{H,j}) + h_{ri} A_{rs,j} (T_{rf,j} - T_{H,j}) + \left(\frac{m_a}{9}\right) c_a (T_{H,y} - T_{H,j}) + \left(\frac{m_a}{9}\right) c_a (T_{H,z} - T_{H,j}) + \left(\frac{m_a}{9}\right) c_a (T_{H,1} - T_{H,j})\right]_{\substack{j=2..9 \\ y=9,2..8 \\ z=3..9,2}} \quad (2)$$

$$\left[(\rho c)_a t_w \frac{dT_{w,j}}{dt} = h_{wo}(T_{amb} - T_{w,j}) + h_{wi}(T_{H,k} - T_{w,j}) + q_{rad,j} - \alpha q_{rerad,j}\right]_{\substack{j=1..8 \\ k=2..9}} \quad (3)$$

$$\left[(\rho c)_a t_{rf} \frac{dT_{rf,j}}{dt} = h_{wo}(T_{amb} - T_{rf,j}) + h_{wi}(T_{H,1} - T_{rf,j}) + q_{rad,j} - \alpha q_{rerad,j}\right]_{j=1..8} \quad (4)$$

In equation 1, the left side represents the accumulation of heat energy over a period of time (1 h time step), and the right side represents the heat transfer due to mass flow heat flux from adjoining volumes and also through vents and the convective heat transfer from the roof and grain surface. Equation 2 is similar to equation 1 but with the addition of a term for the convective heat transfer from the wall surface. In equations 3 and 4, the left side represents the accumulation of heat energy over a period of time (1 h time step), and the right side represents convective heat transfer from the outside and inside wall and roof surfaces, the heat flux due to solar radiation, and the heat flux due to re-radiation. The roof temperatures for the side and central regions were assumed one in order to avoid additional equations for roof temperatures. The central headspace temperature was used in all roof temperature equations (eight equations). The effect of headspace wall temperature on headspace air temperature was added. Solar radiation and convection heat transfer effect were added appropriately in the equations. Due to non-availability of the velocity profile of mass flow between the control volumes, the mass flow through the vents was assumed to be divided equally among the nine control volumes.

The humidity accumulation in the headspace over a period of time was modeled using the mass balance concept (Casada and Young, 1994; Montross et al., 2002a). Nine mass balance equations were formulated based on the inbound and outbound humidity ratio in each control volume (eqs. 5 and 6):

$$\rho_a V_{c,j} \frac{d\gamma_{H,1}}{dt} = \sum_{i=2}^{9}\left(\frac{m_a}{9}\right)(\gamma_{H,i} - \gamma_{H,1}) + h_{mg} A_{g,k}(\gamma_{g,1} - \gamma_{H,1}) + m_a(\gamma_{amb} - \gamma_{H,1}) \quad (5)$$

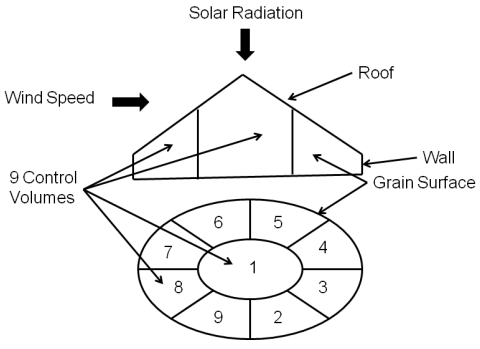

Figure 1. Representation of the headspace model domain.

$$\left[\rho_a V_{s,j} \frac{d\gamma_{H,j}}{dt} = \left(\frac{m_a}{9}\right)(\gamma_{H,1} - \gamma_{H,j}) + \left(\frac{m_a}{9}\right)(\gamma_{H,y} - \gamma_{H,j}) + \left(\frac{m_a}{9}\right)(\gamma_{H,z} - \gamma_{H,j}) + h_{mg} A_{g,j}(\gamma_{g,j} - \gamma_{H,j})\right]_{\substack{j=2..9 \\ y=9,2..8 \\ z=3..9,2}} \quad (6)$$

In equation 5, the left side represents the accumulation of mass (water vapor) over a period of time (1 h time step), while the right side represents the convective mass flux from neighboring volumes, the grain surface, and vents. Equation 6 is similar to equation 5, except for mass flux through vents.

Input Model Parameters

The following input parameters are required to run the developed model: hourly weather data such as ambient temperature and relative humidity, wind speed, solar radiation; volume of each control volume, area of each section of wall, roof and grain surface, emissive and absorptive property of roof material, and convective heat and mass transfer coefficients. The weather data, such as ambient temperature and relative humidity, wind speed, and solar radiation, were downloaded from the Purdue University meteorological website (http://climate.agry.purdue.edu/climate/index.asp).

The convective heat transfer coefficient on the outer silo surface was calculated from wind speed (Montross, 1999). This coefficient was calculated periodically using the equation described by Incropera and Dewitt (2007) and the local wind speed calculated using equation 7. A minimum air velocity of 0.75 m s^{-1} was used whenever the calculated air velocities were below this velocity. Montross (1999) found that during periods of high solar radiation, the convective heat transfer coefficient calculated at low wind velocities (less than 0.75 m s^{-1}) resulted in unrealistically high wall and roof temperatures. Due to lack of better data, the constant convective heat transfer coefficient of 4 W m^2 K^{-1} on the inside wall and roof (Montross, 1999) and the constant convective heat transfer coefficient of 1 W m^2 K^{-1} on the grain surface in the headspace were used in this study, as published by Muir et al. (1980), Maier (1992), and Montross et al. (2002b). Factors such as solar radiation, wind speed, and air infiltration that affect the temperature in the headspace at various locations were assumed constant over 1 h time periods. This assumption was made because historic weather data are typically only available on an hourly basis. The thermal conductivity and viscosity of air were calculated from the ambient air temperature, and the convective heat transfer coefficient around the wall and roof were calculated using equations given by Incropera and Dewitt (2007).

The convective mass transfer coefficient inside the headspace was calculated using the equation described by Incropera and Dewitt (2007). The local wind velocity at bin height was calculated using the following correlation between ambient wind velocity and structural dimensions (Allocca et al., 2003):

$$V_h = 0.35 V_{met} h_b^{0.25} \quad (7)$$

The bin used in this study contains only one vent at the top of the bin. The mass flow enters the headspace through this

0.3 m diameter vent. The infiltration mass flow was calculated as the products of vent area, local wind velocity (volumetric flow), and density of air.

The solar radiation heat flux on the headspace wall and roof, plenum wall, and side wall in contact with the grain mass were calculated using the solar radiation energy balance on these surfaces. The net solar radiation heat flux (q_{rad}) was calculated using the net solar radiation heat flux accumulated on the silo surfaces from absorbing, emitting, and transmitting solar radiation. The net solar radiation heat flux stored on the silo surfaces was the summation of heat flux from earth to silo, sky to silo, from direct radiation, and from diffuse radiation. The equations described by Duffie and Beckman (2006) were used to calculate direct and diffuse solar radiation heat flux on an inclined roof and vertical wall surface. The emissive and absorptive properties of the roof material (GI) were taken as 0.23 and 0.6, respectively (Montross, 1999). Equation details and procedures were given by Lawrence (2010).

This headspace model is part of the overall 3D stored grain ecosystem model. The headspace model was run simultaneously with the 3D grain ecosystem model (Lawrence, 2010). The initial surface grain temperature for the headspace model was taken from the initial grain temperature used in the 3D model. Once the headspace air temperature was determined, this value was used as grain temperature (boundary condition) for the 3D model. This means that the 1 h lagged data of headspace temperature were used as grain temperature in the headspace simulation.

Solution Procedure

The numerical method was used to solve the systems of equations given in equations 1 through 6. The unknown temperature and humidity in each volume depended on the temperature and humidity in the other control volumes, i.e., they are coupled. These coupled equations were solved using the iterative fourth-order Runge Kutta method with the prescribed accuracy limit of 10^{-6}.

Model Validation Procedure

The developed headspace model was validated with field data collected during 1998 and 1999 from silo 12 (2.75 m diameter and 2.9 m eave height with a grain depth of 2.1 m) at the Purdue University PHERC pilot silo facility located at the Agronomy Center for Research and Education, West Lafayette, Indiana. The silo wall, roof, and floor temperatures were measured using thermocouples installed at the four cardinal directions (N, S, E, W) on the inside silo wall surfaces. Silo 12 contained 26 thermistors installed on five cables that monitored hourly grain temperature. In addition, one thermistor was used to monitor the roof surface temperature near the roof peak (south side, 0.9 m from eave) and one relative humidity sensor monitored the headspace air relative humidity and was located on the central section, hanging 0.3 m from the roof. Silo 12 also contained eight thermocouples installed on the headspace inside wall (0.6 m from eave) and roof (0.3 m from eave). The data were logged every hour with a data logger (Fluke Corp., Everett, Wash.). The headspace air temperature and grain surface temperatures were measured using temperature cable thermistors (OPI Systems, Inc., Calgary, Alberta, Canada). One RH sensor was installed in the headspace near the center volume to log RH for comparison with the actual data. A detailed description of this data collection effort is given by Lawrence (2010).

The simulation of the headspace conditions was run for two time periods (May-September 1998 and May-August 1999). Observed data (temperature only) for 1998 were available from July 18 to September 19. Observed data (temperature and RH) for 1999 were available from May 1 to August 31. The standard error was calculated using equation 8 using the hourly predicted and observed temperature and RH values during the time periods given above:

$$SE = \sqrt{\frac{\sum (Y - Y')^2}{n}} \tag{8}$$

The condensation conditions in the headspace were studied by analyzing the headspace air dewpoint temperature and roof temperature. The dewpoint temperature was calculated based on the approximation equations (eqs. 9 and 10) given by Paroscientific (2010):

$$T_d = \frac{b.f(T,RH)}{a - f(T,RH)} \tag{9}$$

$$f(T,RH) = \frac{a.T}{b+T} + \ln(RH) \tag{10}$$

where a = 17.27 and b = 237.7

Results

The headspace model was used to predict the headspace air temperatures and RH, and the wall and roof temperatures. The accuracy of the model was tested by comparing the predicted results with observed data.

Simulation Year 1998

The predicted and observed temperatures in the headspace air, south side roof, and north side wall locations for PHERC silo 12 are given in figures 2 through 4. The prediction for all locations followed the trends of the observed data. However, the model underpredicted the south side roof temperature in the range of 5°C to 10°C during solar radiation peaks and the north side roof temperature in the range of 2°C to 5°C during the nighttime. The standard error of prediction between the observed and predicted headspace temperatures at the center and at the north and south roof and wall locations are given in table 1. For the north side, the model predicted the wall and roof temperatures with standard errors between 2.2°C and 3.1°C lower than for the south side locations.

Simulation Year 1999

The predicted and observed headspace center and south air, south side roof, and north side wall temperatures for PHERC silo 12 from May 1-10, 1999, are given in figures 5 through 8. The predicted temperatures followed the pattern of observed temperature more closely than for simulation year 1998 between night and day. The headspace air temperature varied from 10°C to 40°C, and at the wall and roof it was as high as 60°C. For the south side, the model overpredicted the roof temperature during peak solar days.

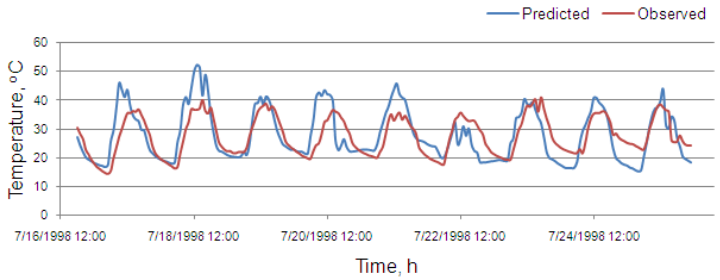

Figure 2. Predicted vs. observed headspace air temperatures in PHERC silo 12 during July 16-26, 1998.

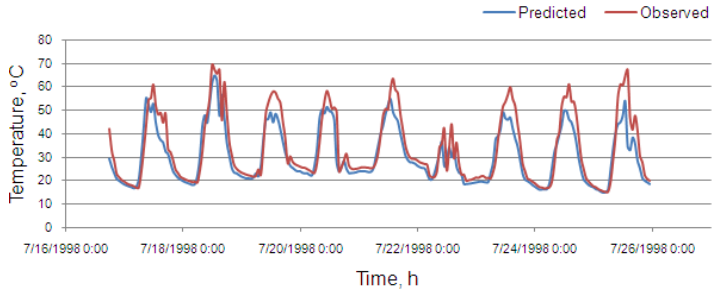

Figure 3. Predicted vs. observed headspace south roof temperatures in PHERC silo 12 during July 16-26, 1998.

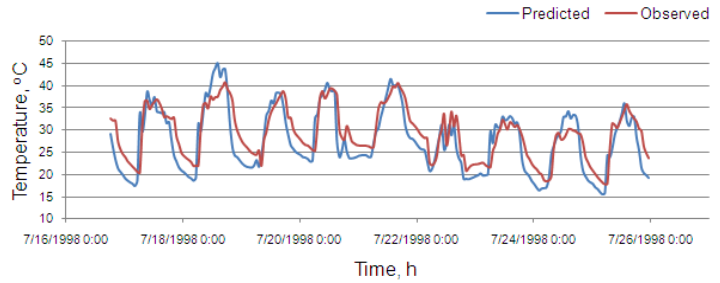

Figure 4. Predicted vs. observed headspace north wall temperatures in PHERC silo 12 during July 16-26, 1998.

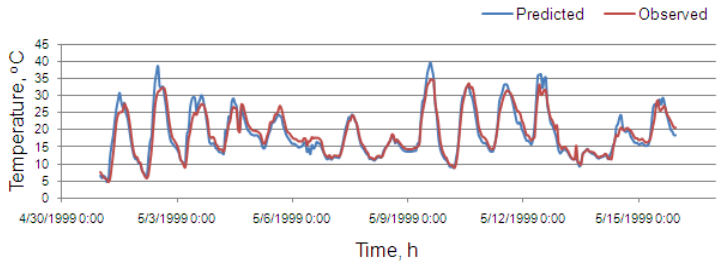

Figure 5. Predicted vs. observed center headspace air temperatures in PHERC silo 12 from May 1-15, 1999.

Table 1. Standard error of prediction (˚C) for the headspace temperature at five locations during July-September 1998.

Headspace Locations	Standard Error (°C)
Center air temperature	5.3
South roof temperature	6.7
North roof temperature	3.6
South wall temperature	5.5
North wall temperature	3.3

The standard errors of prediction between the observed and predicted headspace air, wall, and roof temperatures are given in table 2. The north side roof temperature was predicted with a standard error of 2.3˚C, which was low compared to other locations.

The headspace RH variation during May 1-15, 1999, is given in figure 9. The predicted RH values closely followed the observed values and ranged from 15% to 85%. During the same time period, ambient RH ranged from 25% to 100% (fig. 10). The standard error of prediction between observed and predicted headspace relative humidity values was 7%. For some upper and lower peak periods, the deviation between the predicted and observed RH was 2% to 10%. A relative humidity lag of 2% to 5% was observed in some cycles. The dewpoint temperatures calculated using the observed and predicted headspace air conditions are given in figure 11. The predicted dewpoint temperature mostly followed the trends of the observed dewpoint temperature, but a deviation of up to 2˚C to 7˚C was noticed. The

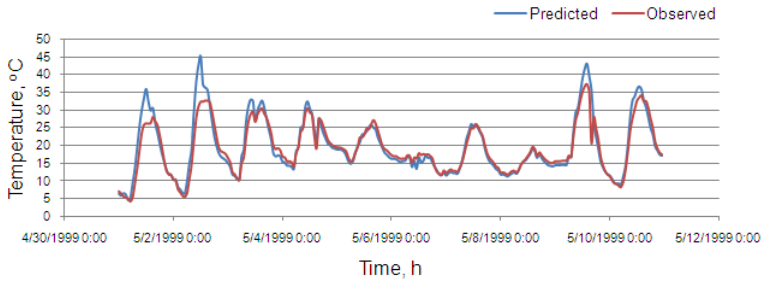

Figure 6. Predicted vs. observed south headspace air temperatures in PHERC silo 12 from May 1-10, 1999.

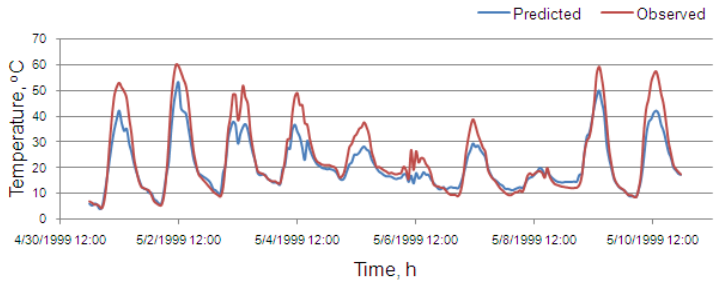

Figure 7. Predicted vs. observed south roof headspace temperatures in PHERC silo 12 from May 1-10, 1999.

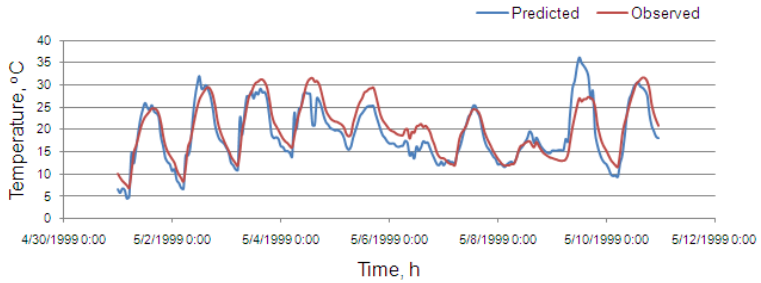

Figure 8. Predicted vs. observed north wall headspace temperatures in PHERC silo 12 from May 1-10, 1999.

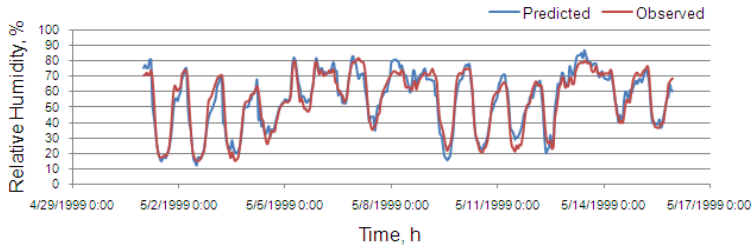

Figure 9. Predicted vs. observed headspace relative humidity in PHERC silo 12 from May 1-15, 1999.

Table 2. Standard error for the headspace temperatures at seven locations during May-August, 1999.

Headspace Locations	Standard Error (°C)
Center air temperature	2.8
South air temperature	3.0
North air temperature	2.3
South roof temperature	5.9
North roof temperature	2.3
South wall temperature	4.2
North wall temperature	3.1

predicted south roof temperature and headspace air dewpoint temperatures are given in figure 12. The roof temperatures of the south locations did not reach the headspace air dewpoint temperature during May 1-31, 1999. This implies that conditions were not sufficiently extreme to cause condensation of moisture in the headspace.

DISCUSSION

In general, the primary effect on headspace temperature was solar radiation. This became evident in the challenge of predicting headspace air, roof, and wall temperatures during the peak solar period of each day. During the day, the headspace air and wall temperatures increased due to solar radiation and then decreased as the intensity of solar radiation diminished during the evening. This pattern was observed in all scenarios and all simulation years. The solar radiation heat flux varied from 0 to 1100 W m^{-2} on a day with the highest

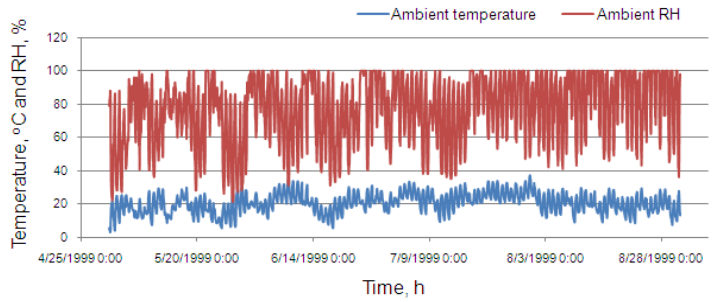

Figure 10. Ambient temperature and relative humidity at the PHERC silo 12 from May 1-15, 1999.

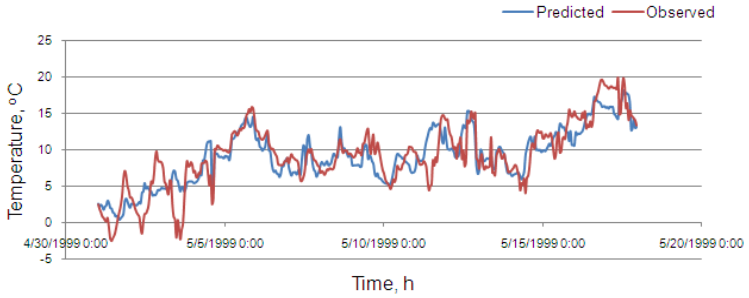

Figure 11. Predicted vs. observed calculated dewpoint temperature in the PHERC silo 12 during May 1-15, 1999.

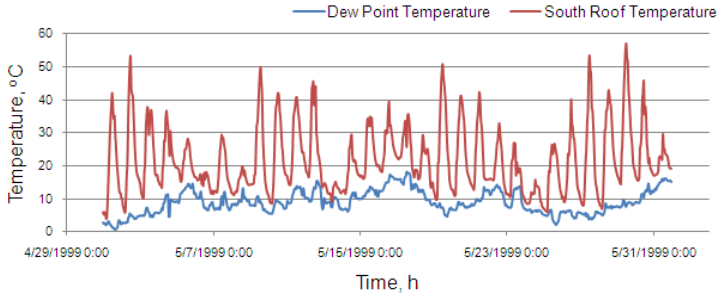

Figure 12. Predicted dewpoint temperatures (using predicted values) vs. south roof temperatures in the PHERC silo 12 during May 1-31, 1999.

radiation intensities observed between 12:00 and 2:00 p.m. The effect of solar radiation varied as a function of azimuth angle. In some instances, south side air temperatures were overpredicted whereas north side air temperatures were underpredicted. This was likely due to the fact that variation in the solar radiation calculation was not captured sufficiently well by only four control volumes with four different solar radiation flux values between the south and north directions. The results indicate that more control volumes may be required to capture the small temperature variations better (Segerlind, 1975). However, working with large numbers of control volumes using this technique would be cumbersome in terms of formulating the equations.

Another possible reason for the over- and underprediction of the effect of solar radiation peaks on headspace air temperature was likely the assumption of constant heat transfer coefficients inside the headspace domain. This assumption was made because no actual momentum transfer data were available. Constant heat transfer coefficients of 4 W m^{-2} K^{-1} for internal wall and roof surfaces and 1 W m^{-2} K^{-1} for the grain surface were used in the model based on previous research (Montross et al., 2002b) but likely did not represent the actual values sufficiently well. The heat transfer coefficient for an outside surface was calculated using the equations given by Incropera and Dewitt (2007) based on wind speed. At times, the calculated convective heat transfer coefficient was too low when wind speed was below the minimum value. During those times, the wall temperature increased abnormally high when compared to observed values. In order to avoid this error, minimum wind speeds of 0.75 m s^{-1} during morning and evening hours and 1.25 m s^{-1} during the solar noon period were specified when the wind speeds dropped below these respective values (Montross et al., 2002b).

The greater standard error in predicting south and north side headspace wall temperatures might have resulted from the variations caused by the wind effect on the wall associated with direction. The direction of wind speed was not taken into account while formulating this model. Instead, wind speed was assumed uniform in all directions. In reality, changes in wind speed direction affect the convective heat transfer coefficient on respective sections of silo wall surfaces. The predicted center headspace air temperature closely followed the observed air temperature, although some deviations were observed during daytime peaks and nighttime valleys. While it can be assumed that much of the deviation was caused by the solar radiation effect, some deviation might also be caused by the variation of mass flow

rate through eave and vent openings and influence of ambient conditions.

Another factor to consider is the solar absorption and emissive properties. These properties for galvanized steel under weathered conditions of silo material are different from new galvanized steel. Montross et al. (2002b) found that a 0.7˚C temperature difference was observed in the predicted values when comparing new and weathered steel properties used in simulations. Properties for new galvanized steel likely also influenced the calculation of solar radiation heat flux on the wall. Casada and Young (1994) suggested that the overprediction of temperature on the silo wall and roof may be due to the fact that the calculated solar heat flux did not adequately represent the difference between clear sky and cloud cover.

There are several possible explanations for the high error in predicting the headspace air RH. The first reason is the use of empirical equations to find the incoming and outgoing mass flow rates in the headspace. The mass flow rate calculated using the empirical equations may not be sufficient to represent the actual scenario during some periods. The second reason is the non-availability of appropriate convective mass transfer coefficient values. In the model, the general equation used to calculate the convective mass transfer coefficient for air on a water surface (Montross et al., 2002b) may not be applicable to calculate the mass transfer between air and the grain surface. In addition, Montross (1999) found that sudden changes in weather pattern over a period of an hour increased the prediction error of the model.

It was further observed that the headspace RH at night was slightly lower than ambient RH. The airflow from the grain surface into the headspace during the nighttime kept the headspace temperature warmer than ambient conditions. It is interesting to note that air conditions during the periods more closely analyzed were such that air humidity was not high enough to cause condensation on the underside of the roof. The deviation in the predicted dewpoint temperature depended mainly on the predicted headspace RH and temperature. Predicted headspace air temperatures were within the range of 2.3˚C to 5.3˚C of the observed values, and predicted headspace roof and wall temperatures were in the range of 2.3˚C to 6.7˚C of the observed values in all simulations. The predicted results were comparable to related research work by Montross (1999) and Casada and Young (1994). Although the errors caused deviations in temperature during the solar peaks and valleys similar to results reported by other researchers, in general the predicted values followed the trends of the observed data measured during the time period. This sufficiently validated the headspace model for a partially filled stored grain silo studied in this research.

Conclusions

A headspace model for a partially filled stored grain silo was developed for a comprehensive 3D stored grain ecosystem using energy and mass balance principles and validated with data collected from the PHERC silos at Purdue University. The conclusions obtained by this study are:

- The predicted headspace air, wall, and roof temperatures followed the trend of the observed values with an acceptable standard error of prediction. The standard error of prediction of the headspace air, wall, and roof temperatures was in the range of 2.3˚C to 5.3˚C, 3.1˚C to 5.5˚C, and 2.3˚C to 6.7˚C, respectively, during 1998 and 1999.
- The predicted headspace RH was well in accordance with the observed headspace values. The standard error between the predicted and observed headspace RH was 7% during 1999.

As a result of this validation, the developed headspace model can be used reliably to predict headspace temperatures and relative humidities in partially filled stored grain silos. This headspace model can be included into the grain storage model to accurately predict the surface grain temperature and moisture content using predicted headspace temperatures and RH as boundary conditions.

Acknowledgements

The information contained in this publication was generated as part of a large-scale, long-term effort between Purdue University, Kansas State University, Oklahoma State University, and the USDA-ARS Grain Marketing and Production Research Center funded by the USDA-CSREES Risk Assessment and Mitigation Program (RAMP), Project No. S05035, entitled “Consortium for Integrated Management of Stored Product Insect Pests.” The project’s goal was to investigate and develop alternative prevention, monitoring, sampling, and suppression measures for organophosphate insecticides used directly on post-harvest grains, which are under scrutiny as a result of the U.S. Food Quality Protection Act (FQPA), and for methyl bromide, which can only be used as a fumigant for pest control in U.S. grain processing facilities under Critical Use Exemption (CUE) as a result of the Montreal Protocol. The collaboration and participation of grain producers, handlers, and processors as well as numerous equipment and service suppliers in this project across the U.S. is greatly appreciated.

References

Allocca, C., Q. Chen, and L. R. Glicksman. 2003. Design analysis of single-sided natural ventilation. *Energy and Buildings* 35(8): 785-795.

Casada, M. E., and J. H. Young. 1994. Model for heat and moisture transfer in arbitrarily shaped two-dimensional porous media. *Trans. ASAE* 37(6): 1927-1938.

Duffie, J. A., and W. A. Beckman. 2006. *Solar Engineering of Thermal Processes.* New York, N.Y.: John Wiley and Sons.

Incropera, F. P., and D. P. Dewitt. 2007. *Fundamentals of Heat and Mass Transfer.* New York, N.Y.: John Wiley and Sons.

Kaliyan, N., R. V. Morey, and W. F. Wilcke. 2005. Mathematical model for simulating the headspace and grain temperatures in grain bins. *Trans. ASAE* 48(5): 1851-1863.

Lawrence, J. 2010. Three-dimensional transient heat, mass, momentum, and species transfer stored grain ecosystem model using the finite element method. PhD diss. West Lafayette, Ind.: Purdue University.

Maier, D. E. 1992. The chilled aeration and storage of cereal grains. PhD diss. East Lansing, Mich.: Michigan State University.

Montross, M. D. 1999. Finite-element modeling of stored grain ecosystems and alternative pest-control techniques. PhD diss. West Lafayette, Ind.: Purdue University.

Montross, M. D., D. E. Maier, and K. Haghighi. 2002a. Development of a finite-element stored grain ecosystem model. *Trans. ASAE* 45(5): 1455-1464.

Montross, M. D., D. E. Maier, and K. Haghighi. 2002b. Validation of a finite-element stored grain ecosystem model. *Trans. ASAE* 45(5): 1465-1474.

Muir, W. E., B. M. Fraser, and R. N. Sinha. 1980. Simulation model of two-dimensional heat transfer in controlled-atmosphere grain bins. In *Controlled Atmosphere Storage of Grains*, 385-398. J. Shejbal, ed. Amsterdam, The Netherlands: Elsevier Scientific.

Nguyen, T. V. 1987. Natural convection effects in stored grains: A simulation study. *Drying Tech.* 5(4): 541-560.

Paroscientific. 2010. MET4 and MET4A calculation of dewpoint. Redmond, Wash.: Paroscientific, Inc. Available at: www.paroscientific.com/dewpoint.htm. Accessed 10 February 2010.

Segerlind, L. J. 1975. *Applied Finite Element Analysis*. New York, N.Y.: John Wiley and Sons.

NOMENCLATURE

A_g = area on the grain surface (m^2)
A_{rs} = area on the roof surface over the side control volume (m^2)
A_{rc} = area on the roof surface over the central control volume (m^2)
A_w = area on the wall surface (m^2)
c_a = specific heat of air (J kg^{-1} K^{-1})
h_b = silo height (m)
h_g = convective heat transfer coefficient on the grain surface (W m^{-2} K^{-1})
h_{mg} = convective mass transfer coefficient on the grain surface (kg m^{-2} s^{-1})
h_{ri} = convective heat transfer coefficient on the roof surface (W m^{-2} K^{-1})
h_{wi} = convective heat transfer coefficient on the inner wall (W m^{-2} K^{-1})
h_{wo} = convective heat transfer coefficient on the outer wall (W m^{-2} K^{-1})
m_a = mass flow from ambient condition (kg s^{-1})
q_{rad} = radiation heat flux (W m^{-2})
q_{rerad} = re-radiation heat flux (W m^{-2})
H = relative humidity (decimal)
T = temperature (˚C)
T_{amb} = ambient air temperature (K)
T_d = dewpoint temperature (˚C)
T_g = grain temperature (˚C)
T_H = headspace air temperature (K)
T_{rf} = headspace roof temperature (K)
t_{rf} = thickness of the roof material (m^2)
t_w = thickness of the wall material (m^2)
u_∞ = ambient wind speed (m s^{-1})
V_c = volume of the center section control volume (m^3)
V_h = local wind velocity (m s^{-1})
V_{met} = meteorological ambient wind speed (m s^{-1})
V_s = volume of the side section control volume (m^3)
α = emissivity of the silo material (decimal)
γ_{amb} = humidity of ambient air (kg H_2O kg^{-1} dry air)
γ_H = humidity of headspace air (kg H_2O kg^{-1} dry air)
γ_g = humidity of headspace grain surface (kg H_2O kg^{-1} dry air)
ρ_a = density of air (kg m^{-3})